Sip1, the *Drosophila* orthologue of EBP50/NHERF1, functions with the sterile 20 family kinase Slik to regulate Moesin activity

Sarah C. Hughes[1,*], Etienne Formstecher[2] and Richard G. Fehon[3]

[1]Department of Medical Genetics, University of Alberta, Edmonton, Alberta, T6G 2H7, Canada
[2]Hybrigenics, 3-5 impasse Reille, 75014 Paris, France
[3]Department of Molecular Genetics and Cell Biology, University of Chicago, Chicago, IL 60637, USA
*Author for correspondence (sarah.hughes@ualberta.ca)

Accepted 4 January 2010
Journal of Cell Science 123, 1099-1107

doi:10.1242/jcs.059469

Summary

Organization of the plasma membrane in polarized epithelial cells is accomplished by the specific localization of transmembrane or membrane-associated proteins, which are often linked to cytoplasmic protein complexes, including the actin cytoskeleton. In this study, we identified Sip1 as a *Drosophila* orthologue of the ezrin-radixin-moesin (ERM) binding protein 50 (EBP50; also known as the Na^+/H^+ exchanger regulatory factor NHERF1). In mammals, EBP50/NHERF1 is a scaffold protein required for the regulation of several transmembrane receptors and downstream signal transduction activity. In *Drosophila*, loss of Sip1 leads to a reduction in Slik kinase protein abundance, loss of Moesin phosphorylation and changes in epithelial structure, including mislocalization of E-cadherin and F-actin. Consistent with these findings, Moesin and Sip1 act synergistically in genetic-interaction experiments, and Sip1 protein abundance is dependent on Moesin. Co-immunoprecipitation experiments indicate that Sip1 forms a complex with both Moesin and Slik. Taken together, these data suggest that Sip1 promotes Slik-dependent phosphorylation of Moesin, and suggests a mechanism for the regulation of Moesin activity within the cell to maintain epithelial integrity.

Key words: FERM domain, Epithelial integrity, Scaffold protein, EBP50/NHERF1, Apical plasma membrane

Introduction

Establishment and maintenance of epithelial integrity through specification of apical-basal cell polarity, organization of the cytoskeleton and establishment of adhesive junctions is essential for the development and function of all metazoans. The cytoskeleton is particularly important for organization of the cell membrane via linkage to transmembrane or membrane-associated proteins. In turn, this organization is required to regulate both epithelial integrity and signaling pathways that control cell fate and cell proliferation. Notably, disruption of epithelial integrity and polarity are initial steps in the progression towards tumorigenesis (Mullin, 2004).

Mammalian ezrin, radixin and moesin (ERM), which are three paralogous proteins, interact with both transmembrane proteins and the actin cytoskeleton within specific domains of the cell cortex to organize the plasma membrane (Amieva et al., 1994; Bretscher, 2002; Franck et al., 1993). Examples of this role include localization of ezrin to apical microvilli in epithelial cells of the developing intestine (Berryman et al., 1993; Berryman et al., 1995; Saotome et al., 2004), enrichment of radixin in the microvilli of liver bile canaliculi (Amieva et al., 1994) and localization of moesin to the membrane of endothelial cells and some polarized epithelial cells (Berryman et al., 1993). ERM proteins include several functional domains including the N-terminal 4.1 ezrin, radixin, moesin (FERM) domain, a coiled-coiled region and a C-terminal actin-binding region (Bretscher, 2002). They are generally thought to have a role in regulating epithelial integrity via linkage with the actin cytoskeleton (Bretscher, 2002; Speck et al., 2003), but other studies also point to a role in regulation of signaling pathways (e.g. RhoA) that control cytoskeletal assembly and organization (Speck et al., 2003). ERM proteins are regulated by intramolecular interactions between the N-terminal FERM domain and C-terminal domain (Bretscher, 2002; Gary and Bretscher, 1993; Gary and Bretscher, 1995; Nguyen et al., 2001), which in turn are regulated in part by changes in phosphorylation (Berryman et al., 1995; Bretscher, 1989; Hirao et al., 1996; Matsui et al., 1998; Matsui et al., 1999; Nakamura et al., 1995; Nakamura et al., 1999; Pietromonaco et al., 1998; Reczek and Bretscher, 1998; Simons et al., 1998). For example, phosphorylation of the conserved C-terminal threonine (T558 in moesin) residue is required for activation of ERM proteins and thus regulates their ability to interact with other binding partners (Matsui et al., 1998). In *Drosophila*, phosphorylation of this conserved Thr residue is dependent on the sterile 20 family kinase Slik (Carreno et al., 2008; Hipfner et al., 2004; Kunda et al., 2008), although the kinase responsible has not been identified definitively in mammalian cells (Belkina et al., 2009; Hipfner et al., 2004; Matsui et al., 1998; Matsui et al., 1999; Oshiro et al., 1998; Pietromonaco et al., 1998; Yokoyama et al., 2005).

EBP50/NHERF1is a membrane-cytoskeletal linking protein that is localized to the apical surface of mammalian epithelial cells (Fouassier et al., 2001; Kreimann et al., 2007; Weinman and Shenolikar, 1993; Weinman et al., 1995). Although originally identified as a regulator of the Na^+/H^+ exchanger, subsequent studies have shown that EBP50/NHERF1 interacts with ERM proteins and can serve as a scaffold to link them to the cytoplasmic tail of transmembrane proteins, as well as to other membrane-associated cytoplasmic proteins such as PDZK1 (Gisler et al., 2003; Morales et al., 2004; Reczek et al., 1997). Thus, EBP50/NHERF1 is believed

to have a key role in ERM-mediated membrane organization. Loss of heterozygosity for EBP50/NHERF1 has been reported to occur in over 50% of breast tumours, and EBP50/NHERF1 mutations are associated with tumour aggressiveness, suggesting that EBP50/NHERF1 has tumour-suppressor functions (Dai et al., 2004; Pan et al., 2006). Interestingly, there is also evidence from breast tumour cell lines that overexpression and mislocalization of ezrin is correlated with invasiveness (Elliott et al., 2005; Sarrio et al., 2006).

To better understand the functional relationship between EBP50/NHERF1 and ERM proteins, we have characterized the role of *Drosophila* Sip1, an EBP50/NHERF1 orthologue. Specifically, we have tested the in vivo functions of Sip1 in relation to the sole ERM orthologue, Moesin, in flies. We show that Sip1 is required for the normal localization and abundance of Slik kinase, the activation of Moesin and the abundance of E-cadherin (Shotgun in *Drosophila*) and F-actin. On the basis of these results, we propose that Sip1 functions with Slik kinase to promote phosphorylation and activation of Moesin to regulate epithelial integrity.

Results

Sip1 is a *Drosophila* orthologue of the mammalian EBP50/NHERF1 protein

Sip1 was identified in a yeast two-hybrid interaction screen (Formstecher et al., 2005) as a protein that binds to a Moesin construct containing either the FERM domain alone or to one that lacks the C-terminal actin-binding domain. The interacting region of Sip1 delineated by interaction with the two Moesin fragments corresponds to residues 217-296, a region that is C-terminal to the PDZ domain of Sip1 (Fig. 1). This interaction domain was defined as the region of overlap of a total of 13 Sip1 clones found in the two screens (data not shown).

A BLAST (Altschul et al., 1990) search of the human protein Refseq database using the *Drosophila* Sip1 protein sequence as a query reported that the closest human homologues were EBP50/NHERF1 and NHERF2. *Drosophila* Sip1 was slightly more similar to human NHERF1 based on the fact that the single PDZ domain in Sip1 is 57% identical and 81% similar to EBP50/NHERF1 PDZ domain 2, compared with 45% identical and 60% similar to human EBP50/NHERF1 PDZ domain 1 (Fig. 1). By comparison, *Drosophila* Sip1 was 53% identical (73% similar) and 40% identical (57% similar) to human NHERF2 PDZ domain 2 and domain 1, respectively (Fig. 1). A reciprocal BLAST search, using the human EBP50/NHERF1 against the *Drosophila* protein database, found that Sip1 had the most significant alignments. A sequence alignment of the PDZ domain of Sip1 was compared with PDZ1 and PDZ2 domains from human, mouse, rat and *Caenorhabditis elegans* (supplementary material Fig. S1). The C-terminal region or 'EB domain' of EBP50/NHERF1, which has previously been shown to bind ezrin in mammals (Fig. 1) (Finnerty et al., 2004; Reczek and Bretscher, 1998) is also conserved in Sip1. There was 23% identity (61% similarity) between the EB domain of Sip1 and human EBP50/NHERF1 (Fig. 1 and supplementary material Fig. S1). There was 28% identity (67% similarity) between the EB domain of Sip1 and human NHERF2 (Fig. 1). The high degree of similarity in the PDZ and EB domains suggests that Sip1 is a *Drosophila* orthologue of EBP50/NHERF1 and that these domains in Sip1 will probably adopt similar structures to their mammalian counterparts.

We identified a P-element insertion allele, $Sip1^{06373}$ (Spradling et al., 1999) that displays homozygous lethality just before, or shortly after, embryonic hatching to the larval state. Animals homozygous

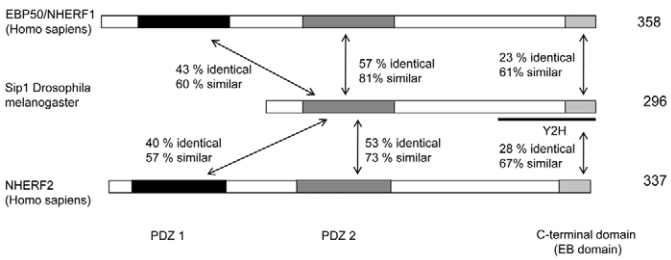

Fig. 1. A comparison of the domain composition of the *Drosophila* Sip1 (NP_524712) protein with human EBP50/NHERF1 (NP_004243) and NHERF2 (NP_001123484). *Drosophila* Sip1 (CG10939) contains only a single N-terminal PDZ domain (shaded region), which is most similar to the second PDZ domain in human EBP50/NHERF1. The percentage amino acid identity and similarity are indicated between the PDZ domains by vertical arrows. The percentage identity and similarity between the EB domain of Sip1 and human EBP50/NHERF1 is indicated by vertical arrows. The C-terminal FERM-binding domain also appears to be conserved. The interacting domain as determined by overlapping clones from the two-hybrid interaction of Sip1 and Moesin is indicated by the dark horizontal line (Y2H).

for the $Sip1^{06373}$ allele are fully rescued to the adult stage by expressing a *UAS-Sip1* transgene under the control of the *T80Gal4* driver. *T80Gal4* is expressed ubiquitously throughout development starting at embryonic stage 11 (Hrdlicka et al., 2002). This result suggests that the P-element insertion specifically affects *Sip1* function.

To better examine Sip1 function, we raised a polyclonal antibody that specifically recognizes this protein (Fig. 2). Within the developing embryonic epithelia, Sip1 partially overlaps with the plasma membrane with some cytoplasmic staining. In contrast to the septate junction marker coracle, Sip1 is not highly associated with the plasma membrane (Fig. 2A-C). Sip1 staining was not apparent in $Sip1^{06373}$ embryos (Fig. 2D-F) indicating that this is a strongly inactivating mutation and that the antibody is specific to Sip1 protein. Upon immunoblot analysis, Sip1 protein was found to be absent in $Sip1^{06373}$ embryos (data not shown). Interestingly, we observed very intense Sip1 staining in the apical region of the hindgut epithelium, which was reminiscent of the expression pattern of EBP50/NHERF1 in renal epithelial cells (Ingraffea et al., 2002; Morales et al., 2004) (Fig. 2G-I). Similarly, in the wing imaginal epithelium, Sip1 was localized apically and overlapped with F-actin staining (Fig. 2J-L). In embryos, Sip1 and Moesin staining overlapped at the apical membrane, as would be expected if these two proteins interact (Fig. 2M-O). Sip1 protein was also localized to the apical membrane in epithelial follicle cells (supplementary material Fig. S2A-C) and colocalized with the pattern of phosphorylated Moesin staining (supplementary material Fig. S2).

Genetic interactions between Sip1 and Moesin

To investigate the functional relationship between *Sip1* and *Moe* (the gene encoding Moesin) we tested genetic interactions between mutations of *Sip1* and *Moe*. Expression of a *UAS-Moe* transgene under control of the *MS1096 GAL4* driver, which is expressed throughout the dorsal surface of the wing, had no discernable phenotype (Fig. 3B). However, when a UAS-inducible *Sip1* expression line, *EP2037*, was expressed using this Gal4 driver, cuticular vesicles were formed along the L3 wing vein (Fig. 3E, arrowhead) and some ectopic vein material was observed (Fig. 3E, arrow). These vesicles suggest that cells expressing *Sip1* are

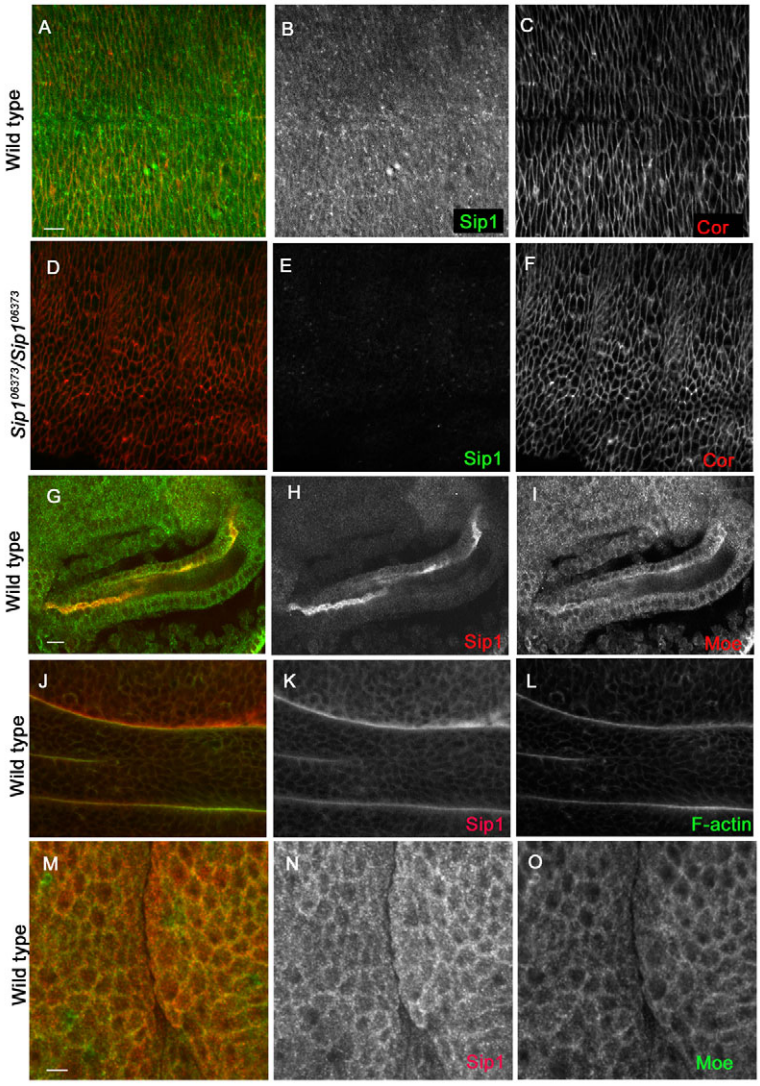

Fig. 2. Sip1 protein localization. Wild type (**A-C**) and *Sip1* mutant (*Sip1*^{06373}, **D-F**) embryos (12-14 hours after egg laying). Sip1 staining is lost in *Sip1* embryos (E), suggesting that this *Sip1* allele is a null mutation and that the antibody is specific. The gain and black level settings are identical in B and E. (**G-I**) Within the embryonic hindgut, there is bright Sip1 staining (H) that colocalizes with Moesin at the apical membrane (I). Sip1 protein is also expressed in third instar larval imaginal discs (**K**) where it colocalizes with filamentous actin (**L**) staining, and is apical to coracle (not shown). (**M-O**) Sip1 largely colocalizes with Moesin in the epithelium of embryos (embryo is shown 7-9 hours after egg laying). Scale bars: 10 μm.

extruded from the wing epithelium (Gibson and Perrimon, 2005). Immunoblots and RT-PCR confirmed that the *EP2037* line expressed *Sip1* upon induction, and *UAS-Sip1* transgenic lines give similar phenotypes (data not shown), indicating that these phenotypes are a consequence of *Sip1* overexpression.

We next examined the effects of co-expression of *Sip1* (using the *EP2037* line) and specific *Moe* transgenes that encode either wild type, activated or inactivated forms of the protein (Speck et al., 2003). Expression of either wild-type *Moe* or the inactivated allele *Moe*^{T559A} alone had no dominant phenotype (Fig. 3B,D), whereas expression of the constitutively activated *Moe*^{T559D} allele (Speck et al., 2003) produced wings that had a wild-type vein pattern, but were curved up slightly at the edge, suggesting that the dorsal surface of the wing is reduced in size (Fig. 3C). Co-expression of wild-type *Moe* with *Sip1* moderately enhanced the venation defects observed with *Sip1* alone (Fig. 3F, arrow and arrowhead), and produced wings that were curved upward, as observed with the activated *Moe*^{T559D} allele, suggesting that *Moe* and *Sip1* are synergistic in their functions. Consistent with this hypothesis, co-expression of activated *Moe* (*Moe*^{T559D}) and *Sip1* produced wings that were dramatically smaller in size and displayed large blisters (Fig. 3G, arrow) and cuticular vesicles (Fig. 3G, arrowhead). This effect on wing development was more severe than that observed with expression of either transgene alone. By contrast, co-expression of inactivated *Moe* (*Moe*^{T559A}) and *Sip1* resulted in adult wings that were wild type in appearance (Fig. 3H), suggesting that the functional interaction between Sip1 and Moesin involves phosphorylation at this conserved threonine residue.

We have shown previously that Moesin is required to maintain epithelial integrity, and that it does so by negatively regulating the RhoA signaling pathway (Speck et al., 2003). To further test interactions between *Sip1* and *Moe*, we asked whether *Sip1* was also involved in RhoA regulation by examining the effect of the genetic dosage of *Rho1* (the *Drosophila* RhoA orthologue) on *Sip1* phenotypes. *Sip1*^{06373} homozygotes did not survive past hatching. However, in *Rho1*^{720} heterozygotes, the percentage of *Sip1* mutants surviving to adulthood increased to an average of 27.8±5%, suggesting that *Rho1* and *Sip1* function antagonistically.

Loss of Sip1 leads to defects of the adherens junctions and actin cytoskeleton

We next examined the effects of *Sip1* mutations in developing epithelia. As *Sip1*^{06373} is late embryonic lethal, we used somatic mosaic analysis to remove *Sip1* function in small groups of cells

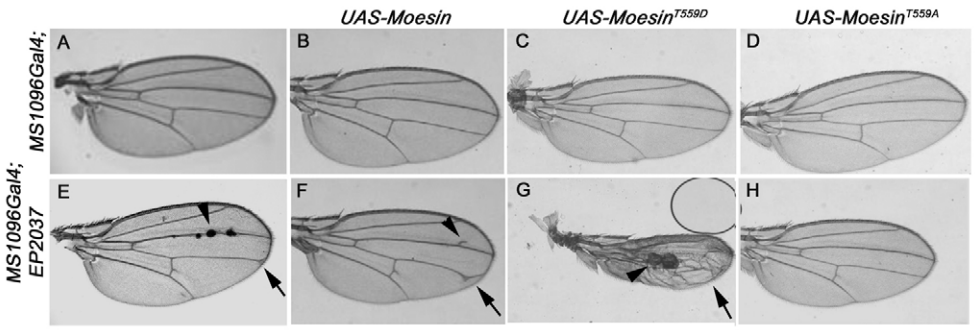

Fig. 3. *Moe* and *Sip1* act synergistically. Expression of either the *MS1096 Gal4* driver alone (**A**), or wild-type *Moe* under the *MS1096 Gal4* driver (**B**), has no apparent affect on adult wing morphology. (**C**) Expression of an activated *Moe* transgene (*UAS- Moe*^{T559D}) produces wings that are curved upwards at the edges (not apparent in this preparation) but otherwise normal. (**D**) Expression of an inactive *Moe* transgene (*UAS-Moe*^{T559A}) results in wings that look completely like the wild type. (**E**) Expression of the *Sip1* EP line, *EP2037*, under the *MS1096 Gal4* driver produces wings with blisters that are apparent along vein L3 (arrowhead) as well as slight venation defects (arrow). (**F**) Co-expression of both *Moe* and *Sip1* (*EP2037*) under control of the *MS1096 GAL4* driver results in wings that have vein defects and are curved upwards at the edges. There is extra vein material on vein L3 (arrowhead) and vein L4 does not reach the wing margin (arrow). (**G**) Co-expression of activated *Moe*^{T559D} and *Sip1* produces wings that are smaller in size and are very warped, with large blister-like (arrow) and vesicle-like structures (arrowhead). (**H**) Co-expression of inactive Moesin (*Moe*^{T559A}) and *Sip1* produces wings that appear normal.

within developing tissues, such as the imaginal discs and the follicular epithelium (Xu and Rubin, 1993). No changes were observed in the relative amount or localization of Moesin (or phosphorylated Moesin), or in the polarity markers E-cadherin and F-actin in imaginal epithelial cells (data not shown). Thus, Sip1 does not appear to be required for Moesin function in these larval tissues, or perhaps has redundant functions with another, unknown, protein.

In contrast to the imaginal disc epithelium, loss of Sip1 function in the follicle cells that surround the developing oocyte and associated nurse cells had severe phenotypes (Fig. 4). Initially, we examined F-actin as a marker for overall cytoskeletal morphology. In wild-type cells, apical F-actin encircled the apical domain in a characteristic honeycomb-like pattern in association with adherens junctions (Fig. 4C). By contrast, in stage 13 follicle cells, F-actin within *Sip1* mutant clones was dramatically redistributed into long fibre-like structures (Fig. 4C, arrow) and E-cadherin staining, a marker for adherens junctions, was strongly reduced (Fig. 4F). We also noted that E-cadherin was depleted on the edges of wild-type cells that border the clonal region (Fig. 4F, arrow) suggesting that the adherens junctions

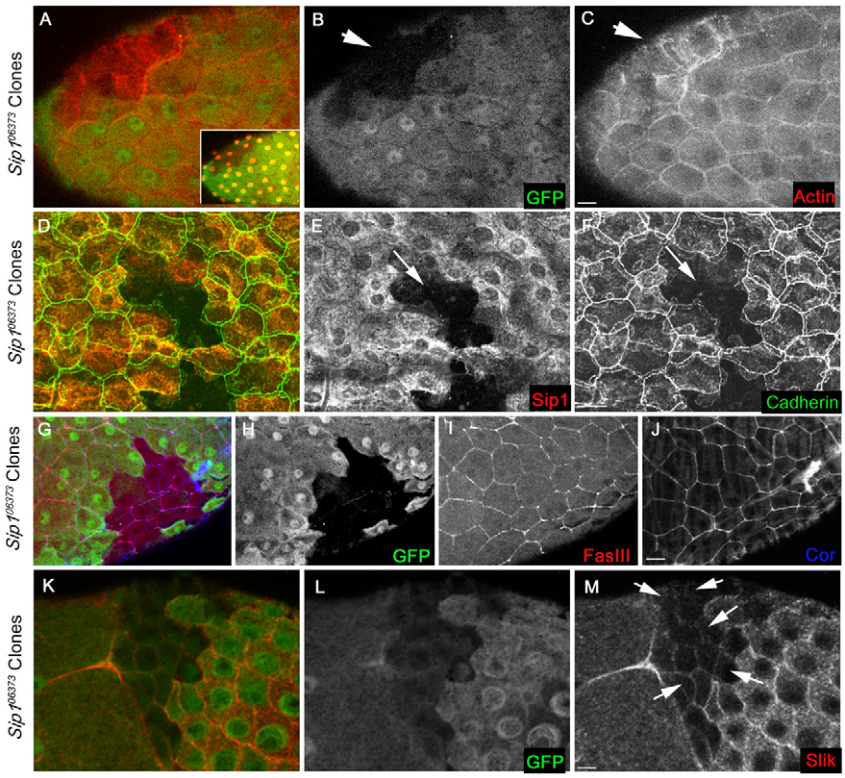

Fig. 4. Loss of *Sip1* expression in the follicle cells surrounding the developing oocyte has dramatic effects on Moesin phosphorylation, filamentous actin organization and localization of Slik. (**A**) Overlay of GFP and phalloidin (F-actin) staining in a stage 13 oocyte. Inset shows DAPI-stained nuclei indicating that cells are present within the *Sip1* mitotic clone. (**B**) *Sip1* clones are identified by the absence of GFP (arrow). (**C**) Phalloidin staining is drastically reorganized into fibre-like structures within each *Sip1* mutant cell. (**D-F**) Stage 13 follicle cells stained with antibodies against Sip1 and E-cadherin. (E) *Sip1* clones are identified by the absence of Sip1 staining (arrow). (F) In *Sip1* mutant clones, E-cadherin labelling of the adherens junctions is lost or mislocalized (arrow). (G-J) Loss of *Sip1* does not affect overall junctional integrity. (**G**) Overlay of a stage 12 oocyte stained for the septate junction markers fasciclin III and coracle. (**H**) *Sip1* clone marked by the absence of GFP. (**I**) Fasciclin III appears unaffected within the clone. (**J**) Coracle staining also appears unchanged within *Sip1* mutant clones. (K-M) *Sip1* is required for normal localization of the Slik kinase. (**K**) Overlay of follicle cells (stage 10) showing GFP and Slik localization. (**L**) The *Sip1* clone is identified by the absence of GFP. (**M**) Within the clone, expression of Slik is reduced and mislocalized (arrows) compared with adjacent wild-type follicle cells. Clones of mutant cells are marked by arrows. Scale bars: 10 μm.

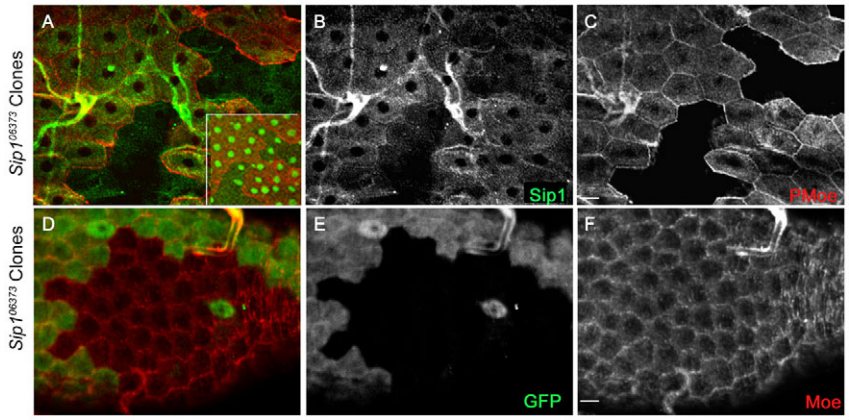

Fig. 5. Sip1 is required for Moesin activation. (**A-C**) Stage 13 follicle cells stained with Sip1 antibodies to label clones and a phospho-specific Moesin antibody to detect active Moesin. Inset shows presence of DAPI-stained (pseudocolored green) nuclei in the clone areas. (B) *Sip1* clones are identified by the absence of Sip1 staining. The TCA fixative used to enhance phospho-Moesin antibody staining in this panel somewhat alters the subcellular localization of Sip1 in wild-type cells. (C) Phospho-Moesin staining is absent within *Sip1* mitotic clones. (**D-F**) Pan anti-Moesin staining is not altered in *Sip1* loss-of-function clones. The clonal region lacking *Sip1* is identified by the absence of GFP (E). Moesin staining appears unchanged in the *Sip1* clone (F). Scale bars: 10 μm.

are also disrupted in borders between wild-type and *Sip1* follicle cells. By contrast, the localization of the septate junction markers coracle and Fasciclin III are not altered in *Sip1* mutant clones (Fig. 4I,J).

Interactions between Sip1, Moesin and Slik

To better understand the functional relationships between Moesin, Slik and Sip1, we examined the effects of mutations in each on the other components in the follicular epithelium. Slik has been shown to regulate the activity of Moesin by controlling phosphorylation of a threonine residue close to the C-terminus (Hipfner et al., 2004). In *Sip1* mutant follicle cell clones, anti-Slik staining was strongly depleted and appeared to be mislocalized relative to adjacent wild-type cells (Fig. 4M). There was less cortical Slik staining and no apparent cytoplasmic Slik staining in *Sip1* mutant cells (Fig. 4M, arrows). These changes in Slik localization were observed from stage 9-10 onward. Consistent with the mislocalization of Slik, activated Moesin staining was absent within *Sip1* mutant clones in stage 13 follicle cells (Fig. 5C), as assayed using a phospho-specific antibody for Moesin (Karagiosis and Ready, 2004). By contrast, a pan-Moesin antibody did not show an obvious change in the abundance of Moesin in *Sip1* mutant cells (Fig. 5F), indicating that Moesin expression and stability are not significantly affected by loss of *Sip1*. These results suggest that Sip1 is required for phosphorylation of Moesin in follicle cells via its effects on Slik localization or stability.

Previous studies have shown that loss of ezrin has a dramatic effect on EBP50/NHERF1 localization in mammalian intestinal epithelia (Saotome et al., 2004). Consistent with the notion that Sip1 is functionally homologous to EBP50/NHERF1, we found that loss of Moesin function had a dramatic effect on the subcellular localization and overall abundance of Sip1within the mutant cells (Fig. 6C). Additionally, loss of Slik resulted in increased staining for Sip1, which appeared to be present not only on the plasma membrane, but also within the cytoplasm of follicle cells (Fig. 6F). The change in the abundance of Sip1 in Slik mutant cells was first apparent at stage 8-9.

The genetic interactions described suggest a complex, interdependent relationship between Moesin, Sip1 and Slik. To examine this further, we used co-immunoprecipitation experiments to ask whether these proteins form complexes in *Drosophila* cultured cells and epithelial tissues. To determine whether Moesin and Sip1 were in a complex, as suggested by the two-hybrid data, we expressed a MYC-tagged *Sip1* transgene in pupal imaginal epithelia and found that it specifically co-immunoprecipitated endogenously expressed Moesin (Fig. 7A). To explore these interactions further, we expressed epitope-tagged Sip1 in cultured S2 cells and found that it specifically pulled down both Moesin and Slik kinase (Fig. 7B), suggesting that both proteins form a complex with Sip1. Taken together with the genetic experiments, these results suggest that Sip1 promoted Moesin function by affecting its interactions with the Slik kinase. Although further experiments will be required to define the precise relationships between these proteins, a possible model for how Sip1 regulates Moesin function is presented in Fig. 8.

Discussion

Previous studies of EBP50/NHERF1 suggested a key role for this protein in regulating transmembrane protein localization and retention at the plasma membrane. In this study, we have taken advantage of the genetic tools available in *Drosophila* to identify and characterize some of the in vivo functions of the EBP50/NHERF1 orthologue Sip1. Searches of the *Drosophila* genome suggest that Sip1 is the single fly orthologue of

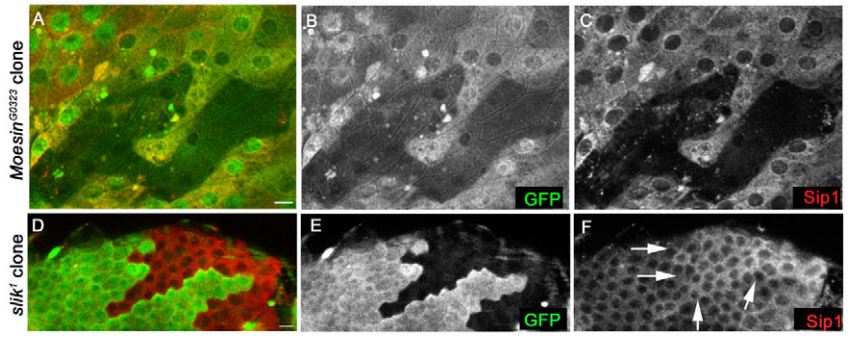

Fig. 6. Loss of Moesin or Slik affects the localization of Sip1 in follicle epithelial cells. (**A-C**) A stage 12 oocyte in which clones of *Moe* mutant cells are identified by the absence of GFP (B). Within the mutant cells, Sip1 staining is strongly reduced (C). (**D-F**) A single confocal section of stage 8 follicle cells with Slik loss-of-function cells identified by the loss of GFP (E). Sip1 staining levels (F) are brighter in the Slik mutant cells (arrows) than in wild-type cells. Scale bars: 10 μm.

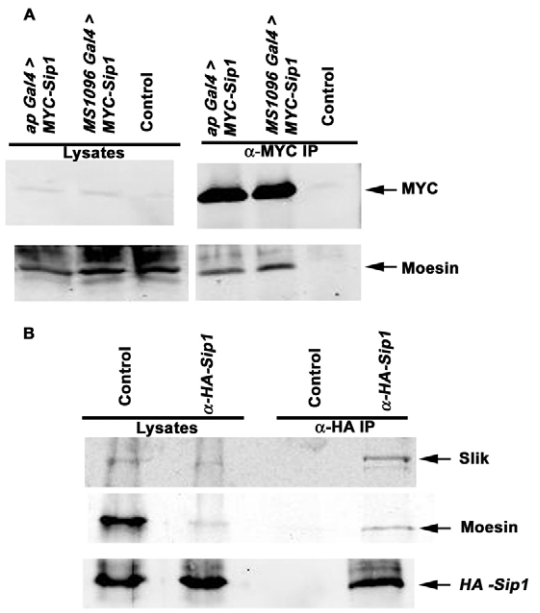

Fig. 7. Sip1, Moesin and Slik proteins interact in vivo. (**A**) A MYC-tagged *Sip1* transgene was expressed under the *apterous Gal4* (*ap Gal4>MYC-Sip1*, lane 1) or *MS1096 Gal4* (*MS1096 Gal4>MYC-Sip1*, lane 2) driver in developing pupal-staged animals. Expressed Sip1 was immunoprecipitated using MYC antibodies. Immunoprecipitates were blotted to detect the presence of co-immunoprecipitated endogenous Moesin protein. The control lane contains a w^{1118}*>MYC-Sip1* lysate mock immunoprecipitated without anti-MYC antibody. Moesin co-immunoprecipitated with Sip1, suggesting that these proteins form a complex in vivo. (**B**) An *UAS HA*-tagged *Sip1* transgene was ubiquitously expressed with *UAS MYC-Moe* and *UAS Slik* in S2 cells. Expressed Sip1 was immunoprecipitated using anti-HA antibody. Immunoprecipitates were immunoblotted to specifically detect both endogenous and transiently expressed Moesin and Slik kinase protein. Co-precipitating Moesin and Slik are observed in the Sip1 immunoprecipitates but not in the mock immunoprecipitate (no HA antibody control) lane.

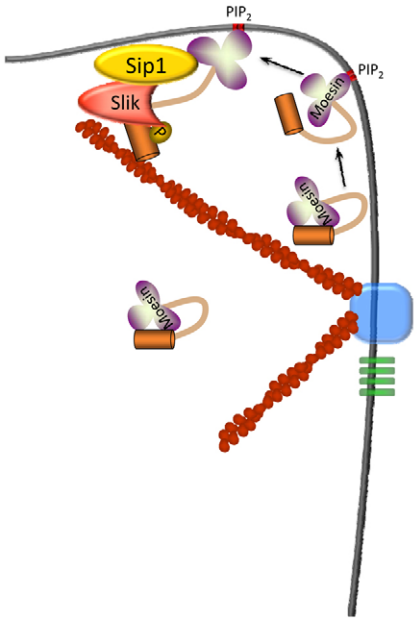

Fig. 8. Possible model for Sip1 in Slik-dependent activation of Moesin. Inactive, folded Moesin in the cell cortex might associate with PIP2 in the plasma membrane, inducing a conformational change that results in partial unfolding of Moesin. This event, or other modifications such as phosphorylation of residues in the FERM domain (Krieg and Hunter, 1992), allow Moesin, Sip1 and Slik to form a complex that results in phosphorylation of the C-terminal Thr residue and full activation of Moesin.

EBP50/NHERF1, whereas in mammals there are two paralogues, EBP50/NHERF1 and NHERF2. Thus studies in *Drosophila* should have fewer potential genetic redundancy problems than those in mammalian systems.

It is interesting to note that the single PDZ domain in Sip1 has higher similarity to human EBP50/NHERF1 PDZ2 (81%) than to PDZ1 (60%). Although differential ligand specificity has been observed between PDZ1 and PDZ2 in EBP50/NHERF1, several ligands, including CFTR, $G_q\alpha$, and SRY-1, appear to bind to both domains (Weinman et al., 2006). Thus, although having a single PDZ domain might decrease the range of ligands to which Sip1 can bind, Sip1 should nonetheless be able to interact with a range of transmembrane and membrane-associated ligands. At this time, we have not yet identified other Sip1 ligands, but it is possible that several PDZ domains in mammals have been adapted to deal with the greater complexity of the mammalian proteome compared with that in flies and worms. However, a clear functional difference is that Sip1 should not be able to act as a scaffold to bring together two ligands, as has been proposed in a few instances for the NHERF proteins (Weinman et al., 2006). Such a function could be provided by other Sip1 binding partners, or might simply not be needed in the fly. Further studies of Sip1 binding partners should address these intriguing questions.

Collectively, our data suggest a novel activity for Sip1, namely that it facilitates Slik-dependent phosphorylation and activation of Moesin. Both genetic and biochemical evidence support this conclusion. Clonal analysis indicates that Sip1 is required for normal subcellular localization and abundance of Slik (Fig. 4M) and normal phosphorylation of Moesin (Fig. 5C) without affecting overall Moesin abundance (Fig. 5F). In addition, Sip1 appears to be upregulated in *slik* mutant cells (Fig. 6F), suggesting that Slik and Sip1 have an interdependent relationship. Co-immunoprecipitation experiments in pupae and in cultured S2 cells indicated that Sip1 forms complexes with both Slik and Moesin, although at the moment it is unclear whether all three proteins are present in a single complex. Taken together, these results suggest that Sip1 functions to bring Slik and Moesin in close proximity, possibly by acting as a scaffold that links these proteins together and leading to phosphorylation of Moesin (Fig. 8). Although our yeast two-hybrid data indicate that Moesin and Sip1 interact directly, we have not distinguished between the possibilities of direct versus indirect interactions with Slik. It is interesting to note that EBP50/NHERF1 has been shown to form a complex with Ste20-related kinase SLK, the mammalian orthologue of Slik, via the adapter protein PDZK1 (Gisler et al., 2003; Lalonde and Bretscher, 2009).

One potential problem with this model is that previous work has suggested that EBP50/NHERF1 is unable to bind the folded, inactive form of ezrin (Finnerty et al., 2004; Reczek and Bretscher, 1998; Morales et al., 2007), raising the question of how Sip1 can facilitate activation of Moesin if it cannot bind the inactive, folded form. A possible answer to this question comes from recent observations that ERMs are regulated by several factors that might operate in a step-wise fashion. Specifically, previous studies have suggested

either a two-step mechanism involving binding of PIP2 to the FERM domain, followed by phosphorylation of the conserved C-terminal Thr (Fievet et al., 2004; Yonemura et al., 2002), or a 'rheostat'-like mechanism that allows for several intermediate states of unfolding and activation (Li et al., 2007). Proposed components of the rheostat mechanism include binding of the FERM domain to PIP2 and phosphorylation, not only of the C-terminal Thr, but of other residues as well. Thus, we propose that interaction of a Sip1-Slik complex with Moesin probably requires previous partial unfolding of Moesin through one or more of these mechanisms (Fig. 8).

Although a role for EBP50/NHERF1 in promoting ERM phosphorylation has not been proposed previously, several aspects of our findings and conclusions are consistent with previous studies in mammalian systems. Sip1 binds Moesin in both two-hybrid and co-immunoprecipitation analyses, as has been observed for EBP50/NHERF1 in mammalian cells (Finnerty et al., 2004; Morales et al., 2004; Morales et al., 2007; Nguyen et al., 2001; Reczek and Bretscher, 1998). Consistent with this result, loss of Moesin and/or ezrin results in mislocalization of Sip1/EBP50 in both the fly and in the mouse (Fig. 6C) (Saotome et al., 2004). In *Ebp50* mutant mice, there is a decrease in phosphorylated ERM proteins in the kidney and intestinal epithelia (Morales et al., 2004). EBP50 is suggested to be necessary to stabilize active phosphorylated ERM proteins at the apical membrane (Morales et al., 2004), but this observation would also be consistent with the model whereby EBP50/Sip1 promotes ERM phosphorylation. Assuming that this is true, what remains unclear is the identity of the responsible kinase in mammalian cells. Although Rho kinase has been proposed to phosphorylate this residue (Matsui et al., 1998; Shaw et al., 1998; Tran Quang et al., 2000), subsequent studies have raised questions about this proposal (Hipfner et al., 2004; Matsui et al., 1999; Takahashi et al., 1997), and no alternative kinase has been identified. The overall conservation of ERMs and Sip1/EBP50/NHERF1 between flies and humans strongly suggests that there is an as yet unidentified sterile 20 kinase family member involved in ERM phosphorylation in mammalian cells.

The requirement of Sip1 for promotion of Moesin activity is also supported by the observation that reduction of the *Rho1* gene dosage partially suppresses the lethality of the *Sip1* mutant animal. Previously, we have shown that Moesin regulates epithelial integrity via downregulation of Rho1 signaling (Speck et al., 2003). Similarly, Slik hypomorphic defects are rescued by a reduced *Rho1* gene dosage (Hipfner et al., 2004), suggesting that Slik regulates Rho1 signaling via phosphorylation and activation of Moesin. Taken together, these results suggest that Sip1, Slik and Moesin function synergistically to negatively regulate Rho1 pathway activity, and emphasize the importance of the functional interaction between Sip1 and Moesin for proper epithelial morphogenesis.

Support for this model comes from the genetic interaction we observed between *Sip1* and *Moe*. Co-expression of an activated *Moe* transgene strongly enhances the effects of *Sip1* expression (Fig. 3G), whereas expression of the inactive, non-phosphorylatable Moe^{T559A} allele suppresses *Sip1* hypermorphic phenotypes (Fig. 3H). These results are consistent with *Sip1* and *Moe* acting synergistically. Furthermore, the observation that the non-phosphorylatable T559A allele suppresses Sip1 expression phenotypes could suggest that co-expression of this form inactivates Sip1, possibly through direct interaction, although we were unable to demonstrate increased complex formation in co-immunoprecipitation experiments (data not shown). In addition, the strong synergistic genetic interactions between *Sip1* and the phosphomimetic form of Moe^{T559D} suggests that Sip1 either interacts specifically with phosphorylated Moesin, or promotes Moesin phosphorylation (Fig. 3G).

It is interesting to note that either reduced or increased levels of Sip1 expression have dramatic effects on epithelial integrity. Loss of function Sip1 clones in follicle cell epithelia result in reorganization of the actin cytoskeleton and loss of E-cadherin localization, strongly suggesting that adherens junction integrity is affected (Fig. 4C,F). In addition, ectopic expression of Sip1 in the adult wing leads to the formation of vesicles (Fig. 3E), which is indicative of defects in cell adhesion (Prout et al., 1997; Walsh and Brown, 1998). In mammalian cells it has also been shown that reduced ezrin levels result in the loss of cell adhesion complexes (Hiscox and Jiang, 1999; Takeuchi et al., 1994). This suggests that the production of Sip1 protein must be tightly regulated within epithelial cells to regulate epithelial integrity, probably through regulation of the interaction between Slik and Moesin.

We consistently observed strong effects of loss of Sip1 function within the follicle cell epithelia, but not in the columnar epithelial cells of third imaginal wing discs, indicating a differential cell requirement for Sip1 activity. This might be linked to changes in cell morphology, because follicle epithelial cells are initially cuboidal, but undergo dramatic changes in cell shape beginning at stage 9. At this point, the follicle cells located over the growing oocyte migrate posteriorly and become columnar, whereas the follicle cells over the nurse cells become squamous (Horne-Badovinac and Bilder, 2005). The majority of the defects that we observed in the follicle cells, whether located over the oocyte or nurse cells, occur at or following, stage 9. These changes in cell shape would require alteration in both cell adhesion and the organization of the actin cytoskeleton, which contribute to the force required for the migration (Horne-Badovinac and Bilder, 2005). Thus, these cells might be particularly susceptible to perturbations that affect regulation of cytoskeletal dynamics or linkage between the plasma membrane and the cytoskeleton. Another, not mutually exclusive, factor is that follicle cells are no longer mitotically active at the stages we observed (Horne-Badovinac and Bilder, 2005), whereas the wing imaginal discs undergo mitosis throughout their development (Milan et al., 1996). Perhaps there are independent mechanisms for regulating the interactions with Slik and Moesin in actively dividing cells. A third possibility is that an unknown protein acts redundantly to Sip1 to regulate the activity of Slik and Moesin in the third instar imaginal disc tissue.

A crucial question that remains to be answered regarding Sip1, Moesin and Slik is how their activities are co-regulated in developing epithelia. Our previous work (Hughes and Fehon, 2006) clearly suggests that regulation of Slik kinase activity is important in developing epithelial cells. The results presented here indicate that the effect of Slik on Moesin activity, and therefore on epithelial integrity, could be regulated by Sip1. Furthermore, because our previous studies have shown that Slik also regulates the tumour suppressor Merlin (Hughes and Fehon, 2006), these results raise the possibility that Sip1 could control proliferation in epithelial tissues. As we can now study the EBP50/NHERF family in *Drosophila*, it should be possible to identify other gene pathways that are involved in the activity and localization of Sip1.

Materials and Methods

Drosophila stocks

The UAS-overexpression line EP2037 was obtained from S. Eaton (EMBL). The UAS-Sip1 transgene was created by subcloning a *Sip1* PCR fragment (5′ primer, CGG GAT CCT CCA CGC CCA CTT CCC CGA AG; 3′ primer, CGC TGC AGT CAG AGC TTC TGA ATG ATG TCG) from the full-length cDNA LD07731 into a

pBS II SK$^+$ N-terminal MYC tag shuttle vector (LaJeunesse et al., 1998). This was subsequently subcloned into a pUAST transformation vector (Brand and Perrimon, 1993). Germline transformation was carried out as described (Rubin and Spradling, 1982) and four independent lines were generated. All other stocks and mutant alleles were obtained from the Bloomington *Drosophila* Stock Center.

Co-immunoprecipitation assays

A mild lysis buffer containing 20 mM HEPES, 50 mM NaCl, 1 mM EDTA, 0.5 mM EGTA, 10 mM DTT, 1% Triton X-100 and protease inhibitors (Complete, Roche) was used for immunoprecipitation. The protein complex associated with MYC epitope-tagged Sip1 protein was immunoprecipitated using an anti-MYC antibody [Developmental Studies Hybridoma Bank (DHSB)] linked to protein-G beads (McCartney and Fehon, 1996) or mouse anti-HA (Sigma) linked to protein-A beads. For the anti-MYC experiment, the control immunoprecipitation uses protein-G beads alone incubated with the respective *Drosophila* lysates, and the control immunoprecipitation with anti-HA Sip1 was performed on transiently transfected Schneider 2 cells, using protein-A beads alone (without anti-HA). Schneider 2 cells were transiently transfected using DDAB (Han, 1996). Lysates for anti-HASip1 immunoprecipitates were crosslinked with 1% formaldehyde upon lysis (Niranjanakumari et al., 2002). Immunoprecipitates were incubated at 4°C for 3 hours, washed extensively in mild lysis buffer, spun down and boiled in 2× SDS sample buffer, run on a 10% SDS-PAGE gel, and transferred to nitrocellulose. Western blot analysis using appropriate primary antibodies (described below) were visualized using an infrared imaging system (Odyssey; LI-COR).

Sip1 antibody production

Polyclonal antibodies recognizing Sip1 were raised in guinea pigs against amino acids 1-296. Sip1 sequences were generated by polymerase chain reaction using the following primers: 5′-CGGGATCCATGTCCACGCCCACTTCCCCG-3′ and 5′-CGGGATCCATGTCCACGCCCACTTCCCCG-3′. This product was excised with *Bam*HI and *Eco*RI and ligated into the corresponding sites of pGEX2. The cloned *Sip1* coding sequence was confirmed by sequencing.

Induction of somatic mosaic clones and immunolocalization

Larvae or female adults of the genotype *42DFRT P(πM)/42DFRT Sip^{06373}; hsFLP/+* or *42DFRT Ubi-GFP^{nls}/42DFRT Sip^{06373}; hsFLP/+* or *42DFRT/42DFRT Sip^{06373}; hsFLP/+* were heat shocked (45 minutes at 37°C, 45 minutes at 25°C, 45 minutes at 37°C) at 36-48 hours after egg laying for the imaginal discs or at 2 days of age for adult females. Larval wing discs were dissected and prepared as described (Hughes and Fehon, 2006). Ovaries from adult females that were 2-4 days post heat shock were dissected in S2 medium and fixed in 4% formaldehyde (Hughes and Fehon, 2006) or 10% trichloroacetic acid (TCA; specifically for the phospho-Moesin staining (Hayashi et al., 1999) or for F-actin (Bateman et al., 2001). Embryos were fixed and prepared for immunofluorescence as described previously (Hughes and Krause, 2001). Antibodies were used as follows: rabbit anti-Moesin D44 at 1:20,000 (D. Kiehart, Duke University, Durham, NC), rabbit anti-phospho-Moesin at 1:10,000 (Karagiosis and Ready, 2004), rabbit anti-phospho ERM (Cell Signaling) (Chorna-Ornan et al., 2005), guinea pig anti-Sip1 at 1:1000 (tissues) or 1:10,000 (immunoblot), guinea pig anti-merlin at 1:10,000 (McCartney and Fehon, 1996), mouse anti-Coracle at 1:500 (Fehon et al., 1994), mouse anti-MYC 9B11 at 1:2000 (Cell Signaling), rat anti-E-cadherin at 1:200 [DCAD2 (Oda et al., 1997)], mouse anti-fasciclin III at 1:1000 (7G10; DHSB) and mouse anti-β-tubulin at 1:5000 (immunoblot; E7, DHSB), mouse anti-MYC (immunoblot; 1:10,000, Cell Signaling) and rat anti-HA at 1:500 (immunoblot; Roche). GFP was visualized directly. Immunostained tissues were mounted in ProLong (Invitrogen) and imaged using either a LSM 410 or LSM 510 confocal microscope (Carl Zeiss MicroImaging) using a plan-Apo ×63, NA 1.4 lens. Figures were compiled in Photoshop 7.0.1 (Adobe).

Analysis of adult wing phenotypes

Flies of the appropriate genotypes were raised at 25°C. Adult wings were prepared as described (LaJeunesse et al., 2001). Images of wings were taken using a Spot RT camera mounted on an Axioplan2ie microscope (Carl Zeiss MicroImaging) using a Fluar ×5, NA 0.25 lens and processed in Photoshop 7.0.1 (Adobe).

We thank A. Simmonds and P. Vanderzalm for comments and critical reading of the manuscript, R. Kulikauskas for preparation of Sip-1 antibody, S. Eaton and the Bloomington Stock Center for fly stocks, D. Kiehart and D. Ready for antibodies, and the Curie-Hybrigenics Laboratory headed by Jacques Camonis. The DCAD2, 7G10 and E7 antibodies were obtained from the Developmental Studies Hybridoma Bank developed under the auspices of the NICHD and maintained by The University of Iowa, Department of Biology, Iowa City, IA 52242. S.C.H. was the recipient of a Young Investigator Award from the Children's Tumour Foundation (formerly known as the National Neurofibromatosis Foundation). This work was supported by a GenHomme Network Grant (02490-6088) to Hybrigenics and Institut Curie and by grant NSOS34783 from the National Institutes of Health to R.G.F. and a grant from the Canadian Breast Cancer Foundation to S.C.H. Deposited in PMC for release after 12 months.

Supplementary material available online at
http://jcs.biologists.org/cgi/content/full/123/7/1099/DC1

References

Altschul, S. F., Gish, W., Miller, W., Myers, E. W. and Lipman, D. J. (1990). Basic local alignment search tool. *J. Mol. Biol.* **215**, 403-410.

Amieva, M. R., Wilgenbus, K. K. and Furthmayr, H. (1994). Radixin is a component of hepatocyte microvilli in situ. *Exp. Cell Res.* **210**, 140-144.

Bateman, J., Reddy, R. S., Saito, H. and Van Vactor, D. (2001). The receptor tyrosine phosphatase Dlar and integrins organize actin filaments in the Drosophila follicular epithelium. *Curr. Biol.* **11**, 1317-1327.

Belkina, N. V., Liu, Y., Hao, J. J., Karasuyama, H. and Shaw, S. (2009). LOK is a major ERM kinase in resting lymphocytes and regulates cytoskeletal rearrangement through ERM phosphorylation. *Proc. Natl. Acad. Sci. USA* **106**, 4707-4712.

Berryman, M., Franck, Z. and Bretscher, A. (1993). Ezrin is concentrated in the apical microvilli of a wide variety of epithelial cells whereas moesin is found primarily in endothelial cells. *J. Cell Sci.* **105**, 1025-1043.

Berryman, M., Gary, R. and Bretscher, A. (1995). Ezrin oligomers are major cytoskeletal components of placental microvilli: a proposal for their involvement in cortical morphogenesis. *J. Cell Biol.* **131**, 1231-1242.

Brand, A. H. and Perrimon, N. (1993). Targeted gene expression as a means of altering cell fates and generating dominant phenotypes. *Development* **118**, 401-415.

Bretscher, A. (1989). Rapid phosphorylation and reorganization of ezrin and spectrin accompany morphological changes induced in A-431 cells by epidermal growth factor. *J. Cell Biol.* **108**, 921-930.

Bretscher, A., Edwards, K. and Fehon, R. G. (2002). ERM proteins and Merlin: Integrators at the cell cortex. *Nat. Rev. Mol. Cell. Biol.* **3**, 586-599.

Carreno, S., Kouranti, I., Glusman, E. S., Fuller, M. T., Echard, A. and Payre, F. (2008). Moesin and its activating kinase Slik are required for cortical stability and microtubule organization in mitotic cells. *J. Cell Biol.* **180**, 739-746.

Chorna-Ornan, I., Tzarfaty, V., Ankri-Eliahoo, G., Joel-Almagor, T., Meyer, N. E., Huber, A., Payre, F. and Minke, B. (2005). Light-regulated interaction of Dmoesin with TRP and TRPL channels is required for maintenance of photoreceptors. *J. Cell Biol.* **171**, 143-152.

Dai, J. L., Wang, L., Sahin, A. A., Broemeling, L. D., Schutte, M. and Pan, Y. (2004). NHERF (Na+/H+ exchanger regulatory factor) gene mutations in human breast cancer. *Oncogene* **23**, 8681-8687.

Elliott, B. E., Meens, J. A., SenGupta, S. K., Louvard, D. and Arpin, M. (2005). The membrane cytoskeletal crosslinker ezrin is required for metastasis of breast carcinoma cells. *Breast Cancer Res.* **7**, R365-R373.

Fehon, R. G., Dawson, I. A. and Artavanis-Tsakonas, S. (1994). A Drosophila homologue of membrane-skeleton protein 4.1 is associated with septate junctions and is encoded by the coracle gene. *Development* **120**, 545-557.

Fievet, B. T., Gautreau, A., Roy, C., Del Maestro, L., Mangeat, P., Louvard, D. and Arpin, M. (2004). Phosphoinositide binding and phosphorylation act sequentially in the activation mechanism of ezrin. *J. Cell Biol.* **164**, 653-659.

Finnerty, C. M., Chambers, D., Ingraffea, J., Faber, H. R., Karplus, P. A. and Bretscher, A. (2004). The EBP50-moesin interaction involves a binding site regulated by direct masking on the FERM domain. *J. Cell Sci.* **117**, 1547-1552.

Formstecher, E., Aresta, S., Collura, V., Hamburger, A., Meil, A., Trehin, A., Reverdy, C., Betin, V., Maire, S., Brun, C. et al. (2005). Protein interaction mapping: a Drosophila case study. *Genome Res.* **15**, 376-384.

Fouassier, L., Duan, C. Y., Feranchak, A. P., Yun, C. H., Sutherland, E., Simon, F., Fitz, J. G. and Doctor, R. B. (2001). Ezrin-radixin-moesin-binding phosphoprotein 50 is expressed at the apical membrane of rat liver epithelia. *Hepatology* **33**, 166-176.

Franck, Z., Gary, R. and Bretscher, A. (1993). Moesin, like ezrin, colocalizes with actin in the cortical cytoskeleton in cultured cells, but its expression is more variable. *J. Cell. Sci.* **105**, 219-231.

Gary, R. and Bretscher, A. (1993). Heterotypic and homotypic associations between ezrin and moesin, two putative membrane-cytoskeletal linking proteins. *Proc. Natl. Acad. Sci. USA* **90**, 10846-10850.

Gary, R. and Bretscher, A. (1995). Ezrin self-association involves binding of an N-terminal domain to a normally masked C-terminal domain that includes the F-actin binding site. *Mol. Biol. Cell* **6**, 1061-1075.

Gibson, M. C. and Perrimon, N. (2005). Extrusion and death of DPP/BMP-compromised epithelial cells in the developing Drosophila wing. *Science* **307**, 1785-1789.

Gisler, S. M., Pribanic, S., Bacic, D., Forrer, P., Gantenbein, A., Sabourin, L. A., Tsuji, A., Zhao, Z. S., Manser, E., Biber, J. et al. (2003). PDZK1: I. a major scaffolder in brush borders of proximal tubular cells. *Kidney Int.* **64**, 1733-1745.

Han, K. (1996). An efficient DDAB-mediated transfection of Drosophila S2 cells. *Nucleic Acids Res.* **24**, 4362-4363.

Hayashi, K., Yonemura, S., Matsui, T. and Tsukita, S. (1999). Immunofluorescence detection of ezrin/radixin/moesin (ERM) proteins with their carboxyl-terminal threonine phosphorylated in cultured cells and tissues. *J. Cell Sci.* **112**, 1149-1158.

Hipfner, D. R., Keller, N. and Cohen, S. M. (2004). Slik Sterile-20 kinase regulates Moesin activity to promote epithelial integrity during tissue growth. *Genes Dev.* **18**, 2243-2248.

Hirao, M., Sato, N., Kondo, T., Yonemura, S., Monden, M., Sasaki, T., Takai, Y. and Tsukita, S. (1996). Regulation mechanism of ERM (ezrin/radixin/moesin) protein/plasma membrane association: possible involvement of phosphatidylinositol turnover and Rho-dependent signaling pathway. *J. Cell Biol.* **135**, 37-51.

Hiscox, S. and Jiang, W. G. (1999). Ezrin regulates cell-cell and cell-matrix adhesion, a possible role with E-cadherin/beta-catenin. *J. Cell Sci.* **112**, 3081-3090.

Horne-Badovinac, S. and Bilder, D. (2005). Mass transit: epithelial morphogenesis in the Drosophila egg chamber. *Dev. Dyn.* **232**, 559-574.

Hrdlicka, L., Gibson, M., Kiger, A., Micchelli, C., Schober, M., Schock, F. and Perrimon, N. (2002). Analysis of twenty-four Gal4 lines in Drosophila melanogaster. *Genesis* **34**, 51-57.

Hughes, S. C. and Krause, H. M. (2001). Establishment and maintenance of parasegmental compartments. *Development* **128**, 1109-1118.

Hughes, S. C. and Fehon, R. G. (2006). Phosphorylation and activity of the tumor suppressor Merlin and the ERM protein Moesin are coordinately regulated by the Slik kinase. *J. Cell Biol.* **175**, 305-313.

Ingraffea, J., Reczek, D. and Bretscher, A. (2002). Distinct cell type-specific expression of scaffolding proteins EBP50 and E3KARP: EBP50 is generally expressed with ezrin in specific epithelia, whereas E3KARP is not. *Eur. J. Cell Biol.* **81**, 61-68.

Karagiosis, S. A. and Ready, D. F. (2004). Moesin contributes an essential structural role in Drosophila photoreceptor morphogenesis. *Development* **131**, 725-732.

Kreimann, E. L., Morales, F. C., de Orbeta-Cruz, J., Takahashi, Y., Adams, H., Liu, T. J., McCrea, P. D. and Georgescu, M. M. (2007). Cortical stabilization of beta-catenin contributes to NHERF1/EBP50 tumor suppressor function. *Oncogene* **26**, 5290-5299.

Krieg, J. and Hunter, T. (1992). Identification of the two major epidermal growth factor-induced tyrosine phosphorylation sites in the microvillar core protein ezrin. *J. Biol. Chem.* **267**, 19258-19265.

Kunda, P., Pelling, A. E., Liu, T. and Baum, B. (2008). Moesin controls cortical rigidity, cell rounding, and spindle morphogenesis during mitosis. *Curr. Biol.* **18**, 91-101.

LaJeunesse, D. R., McCartney, B. M. and Fehon, R. G. (1998). Structural analysis of Drosophila merlin reveals functional domains important for growth control and subcellular localization. *J. Cell Biol.* **141**, 1589-1599.

LaJeunesse, D. R., McCartney, B. M. and Fehon, R. G. (2001). A systematic screen for dominant second-site modifiers of Merlin/NF2 phenotypes reveals an interaction with blistered/DSRF and scribbler. *Genetics* **158**, 667-679.

Lalonde, D. and Bretscher, A. (2009). The scaffold protein PDZK1 undergoes a head-to-tail intramolecular association that negatively regulates its interaction with EBP50. *Biochemistry* **48**, 2261-2271.

Li, Q., Nance, M. R., Kulikauskas, R., Nyberg, K., Fehon, R., Karplus, P. A., Bretscher, A. and Tesmer, J. J. (2007). Self-masking in an intact ERM-merlin protein: an active role for the central alpha-helical domain. *J. Mol Biol.* **365**, 1446-1459.

Matsui, T., Maeda, M., Doi, Y., Yonemura, S., Amano, M., Kaibuchi, K. and Tsukita, S. (1998). Rho-kinase phosphorylates COOH-terminal threonines of ezrin/radixin/moesin (ERM) proteins and regulates their head-to-tail association. *J. Cell Biol.* **140**, 647-657.

Matsui, T., Yonemura, S. and Tsukita, S. (1999). Activation of ERM proteins in vivo by Rho involves phosphatidyl- inositol 4-phosphate 5-kinase and not ROCK kinases. *Curr. Biol.* **9**, 1259-1262.

McCartney, B. M. and Fehon, R. G. (1996). Distinct cellular and subcellular patterns of expression imply distinct functions for the Drosophila homologues of moesin and the neurofibromatosis 2 tumor suppressor, merlin. *J. Cell Biol.* **133**, 843-852.

Milan, M., Campuzano, S. and Garcia-Bellido, A. (1996). Cell cycling and patterned cell proliferation in the wing primordium of Drosophila. *Proc. Natl. Acad. Sci. USA* **93**, 640-645.

Morales, F. C., Takahashi, Y., Kreimann, E. L. and Georgescu, M. M. (2004). Ezrin-radixin-moesin (ERM)-binding phosphoprotein 50 organizes ERM proteins at the apical membrane of polarized epithelia. *Proc. Natl. Acad. Sci. USA* **101**, 17705-17710.

Morales, F. C., Takahashi, Y., Momin, S., Adams, H., Chen, X. and Georgescu, M. M. (2007). NHERF1/EBP50 head-to-tail intramolecular interaction masks association with PDZ domain ligands. *Mol. Cell. Biol.* **27**, 2527-2537.

Mullin, J. M. (2004). Epithelial barriers, compartmentation, and cancer. *Sci. STKE* **2004**, 2.

Nakamura, F., Amieva, M. R. and Furthmayr, H. (1995). Phosphorylation of threonine 558 in the carboxyl-terminal actin-binding domain of moesin by thrombin activation of human platelets. *J. Biol. Chem.* **270**, 31377-31385.

Nakamura, F., Huang, L., Pestonjamasp, K., Luna, E. J. and Furthmayr, H. (1999). Regulation of F-actin binding to platelet moesin in vitro by both phosphorylation of threonine 558 and polyphosphatidylinositides. *Mol. Biol. Cell* **10**, 2669-2685.

Nguyen, R., Reczek, D. and Bretscher, A. (2001). Hierarchy of merlin and ezrin N- and C-terminal domain interactions in homo- and heterotypic associations and their relationship to binding of scaffolding proteins EBP50 and E3KARP. *J. Biol. Chem.* **276**, 7621-7629.

Niranjanakumari, S., Lasda, E., Brazas, R. and Garcia-Blanco, M. A. (2002). Reversible cross-linking combined with immunoprecipitation to study RNA-protein interactions in vivo. *Methods* **26**, 182-190.

Oda, H., Uemura, T. and Takeichi, M. (1997). Phenotypic analysis of null mutants for DE-cadherin and Armadillo in Drosophila ovaries reveals distinct aspects of their functions in cell adhesion and cytoskeletal organization. *Genes Cells* **2**, 29-40.

Oshiro, N., Fukata, Y. and Kaibuchi, K. (1998). Phosphorylation of moesin by rho-associated kinase (Rho-kinase) plays a crucial role in the formation of microvilli-like structures. *J. Biol. Chem.* **273**, 34663-34666.

Pan, Y., Wang, L. and Dai, J. L. (2006). Suppression of breast cancer cell growth by Na+/H+ exchanger regulatory factor 1 (NHERF1). *Breast Cancer Res.* **8**, R63.

Pietromonaco, S. F., Simons, P. C., Altman, A. and Elias, L. (1998). Protein kinase C-theta phosphorylation of moesin in the actin-binding sequence. *J. Biol. Chem.* **273**, 7594-7603.

Prout, M., Damania, Z., Soong, J., Fristrom, D. and Fristrom, J. W. (1997). Autosomal mutations affecting adhesion between wing surfaces in Drosophila melanogaster. *Genetics* **146**, 275-285.

Reczek, D. and Bretscher, A. (1998). The carboxyl-terminal region of EBP50 binds to a site in the amino-terminal domain of ezrin that is masked in the dormant molecule. *J. Biol. Chem.* **273**, 18452-18458.

Reczek, D., Berryman, M. and Bretscher, A. (1997). Identification of EBP50: A PDZ-containing phosphoprotein that associates with members of the ezrin-radixin-moesin family. *J. Cell Biol.* **139**, 169-179.

Rubin, G. M. and Spradling, A. C. (1982). Genetic transformation of Drosophila with transposable element vectors. *Science* **218**, 348-353.

Saotome, I., Curto, M. and McClatchey, A. I. (2004). Ezrin is essential for epithelial organization and villus morphogenesis in the developing intestine. *Dev. Cell* **6**, 855-864.

Sarrio, D., Rodriguez-Pinilla, S. M., Dotor, A., Calero, F., Hardisson, D. and Palacios, J. (2006). Abnormal ezrin localization is associated with clinicopathological features in invasive breast carcinomas. *Breast Cancer Res. Treat.* **98**, 71-79.

Shaw, R. J., Henry, M., Solomon, F. and Jacks, T. (1998). RhoA-dependent phosphorylation and relocalization of ERM proteins into apical membrane/actin protrusions in fibroblasts. *Mol. Biol. Cell* **9**, 403-419.

Simons, P. C., Pietromonaco, S. F., Reczek, D., Bretscher, A. and Elias, L. (1998). C-terminal threonine phosphorylation activates ERM proteins to link the cell's cortical lipid bilayer to the cytoskeleton. *Biochem. Biophys. Res. Commun.* **253**, 561-565.

Speck, O., Hughes, S. C., Noren, N. K., Kulikauskas, R. M. and Fehon, R. G. (2003). Moesin functions antagonistically to the Rho pathway to maintain epithelial integrity. *Nature* **421**, 83-87.

Spradling, A. C., Stern, D., Beaton, A., Rhem, E. J., Laverty, T., Mozden, N., Misra, S. and Rubin, G. M. (1999). The Berkeley Drosophila Genome Project gene disruption project: Single P-element insertions mutating 25% of vital Drosophila genes. *Genetics* **153**, 135-177.

Takahashi, K., Sasaki, T., Mammoto, A., Takaishi, K., Kameyama, T., Tsukita, S. and Takai, Y. (1997). Direct interaction of the Rho GDP dissociation inhibitor with ezrin/radixin/moesin initiates the activation of the Rho small G protein. *J. Biol. Chem.* **272**, 23371-23375.

Takeuchi, K., Sato, N., Kasahara, H., Funayama, N., Nagafuchi, A., Yonemura, S. and Tsukita, S. (1994). Perturbation of cell adhesion and microvilli formation by antisense oligonucleotides to ERM family members. *J. Cell Biol.* **125**, 1371-1384.

Tran Quang, C., Gautreau, A., Arpin, M. and Treisman, R. (2000). Ezrin function is required for ROCK-mediated fibroblast transformation by the net and dbl oncogenes. *EMBO J.* **19**, 4565-4576.

Walsh, E. P. and Brown, N. H. (1998). A screen to identify Drosophila genes required for integrin-mediated adhesion. *Genetics* **150**, 791-805.

Weinman, E. J. and Shenolikar, S. (1993). Regulation of the renal brush border membrane Na(+)-H+ exchanger. *Annu. Rev. Physiol.* **55**, 289-304.

Weinman, E. J., Steplock, D., Wang, Y. and Shenolikar, S. (1995). Characterization of a protein cofactor that mediates protein kinase A regulation of the renal brush border membrane Na(+)-H+ exchanger. *J. Clin. Invest.* **95**, 2143-2149.

Weinman, E. J., Hall, R. A., Friedman, P. A., Liu-Chen, L. Y. and Shenolikar, S. (2006). The association of NHERF adaptor proteins with g protein-coupled receptors and receptor tyrosine kinases. *Annu. Rev. Physiol.* **68**, 491-505.

Xu, T. and Rubin, G. M. (1993). Analysis of genetic mosaics in developing and adult Drosophila tissues. *Development* **117**, 1223-1237.

Yokoyama, T., Goto, H., Izawa, I., Mizutani, H. and Inagaki, M. (2005). Aurora-B and Rho-kinase/ROCK, the two cleavage furrow kinases, independently regulate the progression of cytokinesis: possible existence of a novel cleavage furrow kinase phosphorylates ezrin/radixin/moesin (ERM). *Genes Cells* **10**, 127-137.

Yonemura, S., Matsui, T. and Tsukita, S. (2002). Rho-dependent and -independent activation mechanisms of ezrin/radixin/moesin proteins: an essential role for polyphosphoinositides in vivo. *J. Cell Sci.* **115**, 2569-2580.

Journal of Cell Science